Available online at www.sciencedirect.com
ScienceDirect
Catalysis Today 133–135 (2008) 160–167
CATALYSIS TODAY
www.elsevier.com/locate/cattod

Effect of lanthanum addition on the properties of potassium-free catalysts for ethylbenzene dehydrogenation

Manuela de Santana Santos [a], Sergio Gustavo Marchetti [b], Alberto Albornoz [c], Maria do Carmo Rangel [a,*]

[a] GECCAT Grupo de Estudos em Cinética e Catálise, Instituto de Química, Universidade Federal da Bahia, Campus Universitário de Ondina, Federação. 40 170-280, Salvador, Bahia, Brazil
[b] CINDECA, Facultad de Ciencias Exactas, Universidad Nacional de La Plata 1900, 47 y 115, La Plata, Argentina
[c] Instituto Venezolano de Investigaciones Científicas, Apartado 21 827, Caracas 1920-A, Venezuela

Available online 1 February 2008

Abstract

The ethylbenzene dehydrogenation in the presence of steam is the dominant technology for styrene production, one of the most important high value chemicals. The most widely used industrial catalyst comprises potassium-promoted iron oxide, which deactivates with time, due to potassium loss. In order to find alternative free-potassium catalysts, the effect of lanthanum on hematite-based catalysts was studied in this work. Samples with different amounts of lanthanum and prepared with different precipitants (ammonium hydroxide, sodium carbonate and sodium hydroxide) were obtained. It was found that lanthanum led to the production of solids with small particles when ammonium hydroxide was used, a fact which was assigned to lanthanum species on the surface where they keep the hematite particles apart avoiding sinterization. On the other hand, bigger particles were produced when sodium hydroxide and sodium carbonate are used, which resulted in solids with small specific surface areas. This was related to the sodium species which covered the surface impairing the lanthanum action. The most promising catalyst was that prepared with ammonium hydroxide and with La/Fe = 0.1, which showed the highest specific activity and the highest activity per area. In this solid, lanthanum acts as a structural promoter.

Keywords: Ethylbenzene; Styrene; Lanthanum; Hematite

1. Introduction

Styrene is one of the most important monomer in the modern petrochemical industry, largely used in the production of different polymers, including polystyrene, styrene–acrylonitrile (SAN), acrylonitrile–butadiene–styrene (ABS) and styrene–butadiene latex [1]. Among them, polystyrene consumes the majority of the world production of styrene (more than 50%) for the manufacture of thermal isolation, tubes, latex, plastic accessories and other materials [2].

The styrene monomer can be produced by several routes, such as the catalytic dehydrogenation of ethylbenzene in the presence of superheated steam, the oxidative dehydrogenation of ethylbenzene and the dehydrogenation of ethylbenzene coupling to the water–gas shift reaction [3]. This compound can also be obtained by the catalytic dehydration of methyl-phenyl-carbinol [4,5] or as a co-product, in the manufacture of propylene oxide [1]. Among these processes, the ethylbenzene dehydrogenation in the presence of steam is by far the most important route to produce styrene and is responsible for 90% of the world production of this monomer [6].

In commercial processes, ethylbenzene dehydrogenation is often performed in the range of 530–650 °C and 0.3–1.0 bar, over two catalytic fixed-beds, in adiabatic or isothermal operations [4–10]. From the kinetic point of view, the process involves six reactions, consisting of the main reaction, the formation of aromatic by-products from ethylbenzene by dealkylation and hydrogenolysis, the steam reforming of the resulting methane and ethylene and the water–gas shift reaction [11–13]. The main reaction is highly endothermic and thermodynamically limited and thus the conversion increases with temperature and decreases with the pressure increase.

* Corresponding author.
E-mail address: mcarmov@ufba.br (M. do Carmo Rangel).

0920-5861/$ – see front matter © 2008 Elsevier B.V. All rights reserved.
doi:10.1016/j.cattod.2007.12.052

Steam is often used to provide heat for the reaction, to stabilize the catalyst and to minimize the coke deposition [5,10].

The commercial catalysts used in the ethylbenzene dehydrogenation in the presence of steam comprise iron oxide and promoters like potassium and chromium oxide, among others [4–9]. Potassium increases the iron activity and decreases the coke deposition, while chromium oxide increases the activity and decreases sinterization [7–9]. Although these systems are active and selective, the severe conditions of the industrial processes result in a progressive deterioration, which leads to catalyst replacement each one or two years [13]. As a consequence, a lot of work has been carried out aiming to develop catalysts with high chemical, mechanical and structural stability [5,10,11,14,15].

The main causes of catalyst deactivation during the ethylbenzene dehydrogenation in the presence of steam are the coke deposition, the loss of potassium promoter and the change of oxidation state of iron [10]. In order to avoid these drawbacks, several process conditions were proposed such as high steam to ethylbenzene molar ratio and the use of alkaline metal to promote the gasification of carbonaceous deposits, as well as the addition of several metals, which can stabilize the active oxidation state of iron oxide [4]. However, the most serious problem of deactivation is caused by the loss of potassium, which migrates in two directions, during the life of the catalyst. This promoter can migrate downstream in the water layer of the condensed product and to the center of the catalyst pellets [7,8].

An impressive amount of work has been published, in the last decades, aiming to state the nature of the active phase of the catalyst [10], the role of promoters [4] and also aiming to find alternative catalyst in order to solve the problem of catalyst deactivation [4–8,14–21]. Nevertheless, many industrial problems are still unsolved, which have motivated the search for new potassium-free catalysts, which can work without deactivation.

With this goal in mind, the influence of lanthanum amount on the catalytic and textural properties of iron oxide was investigated in the present work. The effect of the kind of the precipitant agent on the properties of this solid was also evaluated.

2. Experimental

The samples were obtained by the sol–gel method, from lanthanum nitrate, iron nitrate and ammonium hydroxide. The sol was produced by the addition of an iron nitrate solution (1 M, 250 mL), a lanthanum nitrate solution (0.2 M, 250 mL) and an ammonium hydroxide solution (25% (v/v), 250 mL) to a beaker with water, at room temperature, under stirring. After the addition of the reactants, the system was kept under stirring for 30 min and then centrifuged (2000 rpm, 5 min). The gel obtained was rinsed with water and centrifuged several times, until no nitrate ion was detected in the supernatant anymore. The gel was dried in an oven at 120 °C, for 12 h, ground and sieved in 100 mesh. The precursor was heated under nitrogen flow at 600 °C, for 2 h, to produce a sample with a lanthanum to iron molar ratio of 0.2 (LF02 sample). The same procedure was used to prepare the sample with a lanthanum to iron molar ratio of 0.1 (LF01 sample). In this case, an iron nitrate solution (1 M) and a lanthanum nitrate solution (0.1 M) were used. Pure lanthanum oxide (L sample) was also prepared by the same procedure from a lanthanum nitrate solution (1 M, 250 mL) and an ammonium hydroxide solution (8.5% (v/v), 250 mL).

The effect of the kind of the precipitant agent on the catalysts properties was investigated using the most active and selective catalyst towards styrene of the first set of experiments (LF01 sample). The samples were prepared using sodium carbonate or sodium hydroxide, instead of ammonium hydroxide, following the same experimental method. The solids were named LFNC (sodium carbonate) and LFNH (sodium hydroxide). Free-lanthanum samples were also prepared as references.

The precursors were characterized by differential scanning calorimetry (DSC) and thermogravimetry (TG) and the catalysts were characterized by chemical analysis, specific surface area measurements, X-ray diffraction, temperature-programmed reduction (TPR), X-ray photoelectron spectroscopy (XPS) and Mössbauer spectroscopy.

The differential scanning calorimetry (DSC) and thermogravimetry (TG) experiments were performed on the precursors in order to follow the effect of lanthanum and of the precipitant agent on the catalyst production under heating. During the experiments, the sample was heated at 10 °C min^{-1}, under nitrogen flow from 30 °C to 1000 °C, in the case of TG and up to 600 °C, in the case of DSC in Shimadzu models DSC-50 and TG-50 equipments.

The iron contents were determined by X-ray dispersive energy in a Shimadzu model EDX-700HS equipment. The phases in the solids were identified by X-ray diffraction experiments performed at room temperature with a Shimadzu model XD3A instrument, using Cu Kα radiation generated at 30 kV and 20 mA and a nickel filter. The specific surface areas were measured in a Micromeritics model TPR/TPO 2900 equipment on samples previously heated under nitrogen (160 °C, 1 h). The temperature-programmed reduction (TPR) was performed on calcined samples (0.035 g) in a Micromeritics model TPD/TPO 2900 equipment, using a 5% H_2/N_2 mixture. Before the analysis, the samples were heated under nitrogen flow (60 mL min^{-1}) at 10 °C min^{-1} until 160 °C for 30 min.

X-ray photoelectron spectra were obtained with a VG ESCALAB 220i-XL spectrometer equipped with a Mg Kα X-ray radiation source ($h\nu = 1253.6$ eV) and a hemispherical electron analyzer, operating at 400 W. Before the analysis, the samples were outgassed (10^{-10} Torr). The Si2p peak was chosen as an internal reference. This reference was in all cases in good agreement with the BE of the C1s peak, arising from contamination, at 284.9 eV. This reference gave an accuracy of ±0.1 eV.

Mössbauer spectra were obtained with a spectrometer equipped with 12 channels with constant acceleration and geometry of transmission. A source of ^{57}Co was used in a womb of Rh of 50 me normal. All the isomeric shifts were related for a standard at 298 K. The spectra were obtained at room temperature and fitted with a square minimum program, no

line with restrictions. For each component of the spectra, were employed Lorentzians lines of the same width. All the spectra were fitted and were obtained the distributions of the hyperfine parameter for quantify the different phase of the iron oxides.

The catalyst performance was evaluated using 0.3 g of powder and a fixed-bed microreactor, providing there is no diffusion effect. The experiments were carried out at atmospheric pressure under isothermal condition (530 °C), using a feed composition of 2.6% ethylbenzene and 26% steam in nitrogen. The reactor, containing the catalyst, was heated under nitrogen flow (60 mL min^{-1}) up to the reaction temperature. Then the feed was interrupted and the reaction mixture was introduced in the reactor. The reaction mixture was obtained by passing a nitrogen stream through a saturator with ethylbenzene and then through a chamber where it was mixed with steam. The gaseous effluent from the reactor was collected in a condenser and the organic phase was analyzed by gas chromatography, using a CG-35 instrument. In these conditions, 10% of ethylbenzene conversion was obtained over a commercial catalyst. The spent catalysts were characterized by X-ray diffraction, specific surface area measurement, X-ray photoelectron spectroscopy and Mössbauer spectroscopy.

3. Results and discussion

The DSC thermograms of the sample prepared with ammonium hydroxide (Fig. 1) showed an endothermic peak at temperatures bellow 100 °C assigned to the loss of physically adsorbed volatiles on the solids. This effect was followed by weight loss as it can be noted in TG curves. In the pure iron oxide curve, there is an exothermic peak at 450 °C, assigned to hematite crystallization. This effect is not followed by weight loss, in agreement with several data previously reported [22–24]. The precursor of pure lanthana (L sample) showed two endothermic peak in the DSC curves, followed by weight loss. These events can be assigned to the production of lanthanum oxide, from the successive dehydration steps of the lanthanum hydroxide decomposition, as found by other workers [25,26]. In the iron and lanthanum-containing materials, the endothermic peaks were shifted to lower temperature and were less intense as compared to pure iron oxide, since the exothermic effect of hematite crystallization was compensated by the endothermic effect of lanthana dehydration. These shifts indicate that the formation of both hematite and lanthana was delayed as compared to pure oxides, due to the simultaneous presence of iron and lanthanum.

The X-ray diffractograms of the catalysts prepared with ammonium hydroxide are shown in Fig. 2(a). It can be noted the production of hematite, in the free-lanthanum sample, in agreement with the result of thermal analysis. The addition of lanthanum to iron oxide produced a broad peak diffraction probably due to the small size of the particles and/or to the low crystallinity of the solids. It was not detected any lanthanum-containing phase.

Fig. 2(b) shows the X-ray diffractograms of the catalysts, after the catalytic test. It can be noted that a phase transition and the growing of the particles occurred during the ethylbenzene

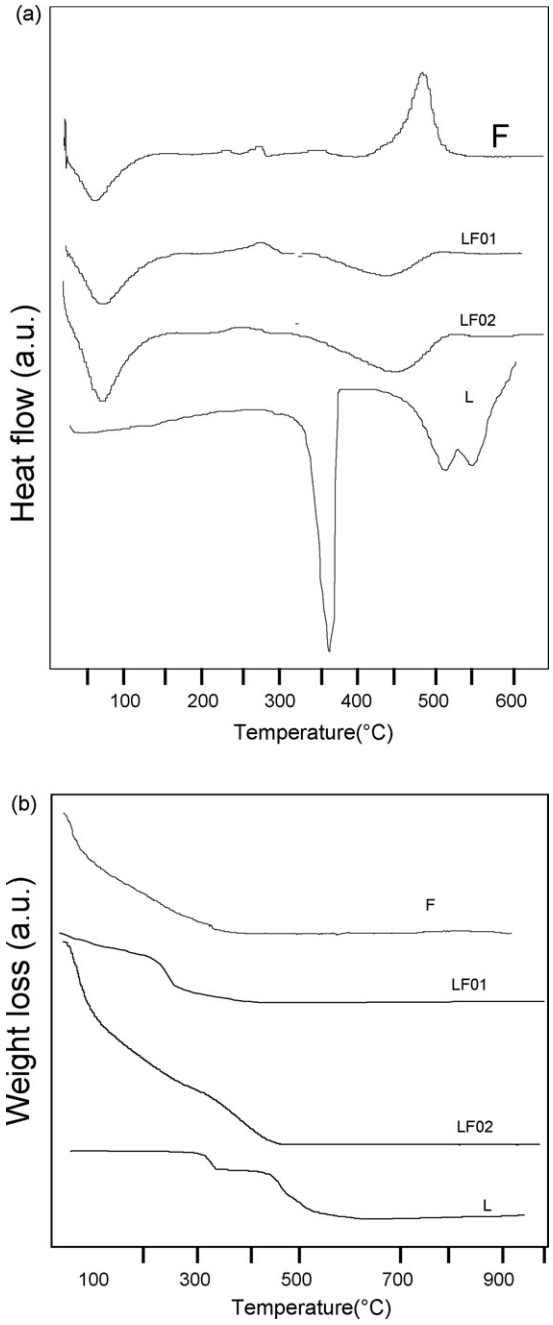

Fig. 1. Curve of differential scanning calorimetry of the catalyst precursors. LF01 and LF02 samples: with La/Fe (molar) = 0.1 and 0.2; F and L samples: pure iron hydroxide and lanthanum hydroxide, respectively.

dehydrogenation. In all cases, magnetite (Fe_3O_4) was produced and the peaks became narrower. Lanthanum oxide was also produced during reaction.

In accordance with these results, the specific surface area decreased during reaction, due to particles growing, as shown in Table 1. We can also see that the addition of lanthanum caused an increase of the specific surface area of the fresh catalysts; the highest value was obtained when small amounts were added. In addition, lanthanum was not able to prevent sintering during reaction, regardless its amount in solids. The role of lanthanum in preventing sintering can be related to its action as a spacer on

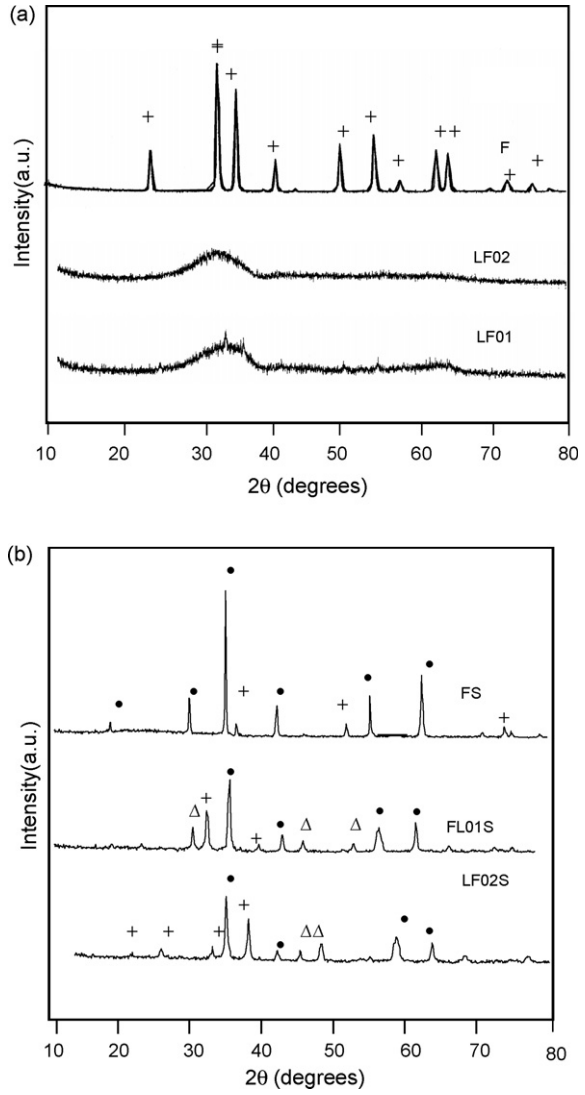

Fig. 2. X-ray diffractograms of the fresh (a) and (b) spent catalysts prepared with ammonium hydroxide. LF01 and LF02 samples: with La/Fe (molar) = 0.1 and 0.2, respectively; F sample: iron oxide, (△) La_2O_3, (+) α-Fe_2O_3 and (●) Fe_3O_4.

the solid surface keeping the particles apart. Due to the large atomic radius of La^{3+} species (1.05 Å), as compared to Fe^{3+} species (0.64 Å), they are expected not to enter in the iron oxide lattice, but to form a segregated phase. This phase was detected only in the spent catalysts, probably due to the small particle size in the fresh catalysts. The DSC and TG results confirmed the production of this phase also in the fresh catalysts.

The catalysts showed similar reduction profiles, regardless the presence and the amount of lanthanum, as shown in Fig. 3.

Table 1
Specific surface area of the catalysts before (Sg) and after the reaction (Sg*)

Samples	Sg ($m^2\ g^{-1}$)	Sg* ($m^2\ g^{-1}$)
F	17	11
LF01	115	10
LF02	97	12

LF01 and LF02 samples: with La/Fe (molar) = 0.1 and 0.2, respectively; F sample: pure iron oxide.

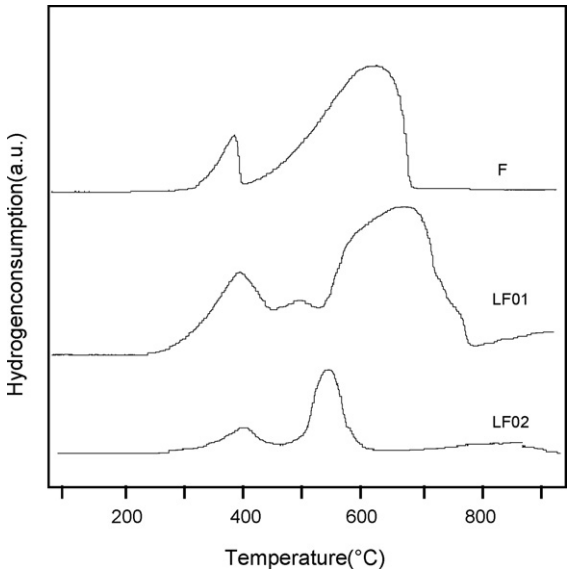

Fig. 3. Temperature-programmed reduction curves of the catalysts prepared with ammonium hydroxide. LF01 and LF02 samples: with La/Fe (molar) = 0.1 and 0.2, respectively; F sample: iron oxide.

The F sample displayed peaks beginning at 310 °C and 405 °C. According to literatures [23,27–29] the first one is assigned to the reduction of hematite (α-Fe_2O_3) to magnetite (Fe_3O_4) while the broad peak at high temperatures is related to the reduction of magnetite to produce metallic iron. The reduction is supposed to proceed through the following reaction steps [29]:

$$H_2 + 3\alpha\text{-}Fe_2O_3 \rightarrow 2Fe_3O_4 + H_2O \quad (1)$$

$$4H_2 + Fe_3O_4 \rightarrow 3\alpha\text{-}Fe + 4H_2O \quad (2)$$

By adding lanthanum, the reduction started at lower temperatures regardless the amount of lanthanum in solids. The high temperature peak was also affected by lanthanum; the maximum of the LF01 sample was shifted to a high temperature whereas the maximum of the LF02 sample was shifted to a lower temperature. The LF01 sample showed also an intermediate peak which can be related to the magnetite reduction on the particle surface. These results showed that lanthanum affected both hematite and magnetite reduction.

All catalysts were active in ethylbenzene dehydrogenation and selective towards styrene, reaching stable values, after about 3 h of reaction, as showed in Fig. 4. The average values after this period are shown in Table 2. It can be seen that lanthanum largely improved the catalysts, increasing the conversion; this can be assigned to an increase of activity per area and then lanthanum acts as a structural promoter. The styrene selectivity decreased due to lanthanum, but the styrene yield increased. It also can be seen that the activity and selectivity increased with the amount of lanthanum in solids. All catalysts showed low production of toluene and benzene, the main by-products of reaction, as shown in Table 2.

The catalyst with lanthanum to iron molar ratio of 0.1 (LF01 sample) showed the best performance in the ethylbenzene dehydrogenation to produce styrene, presenting an activity about three times higher than pure hematite. This sample was

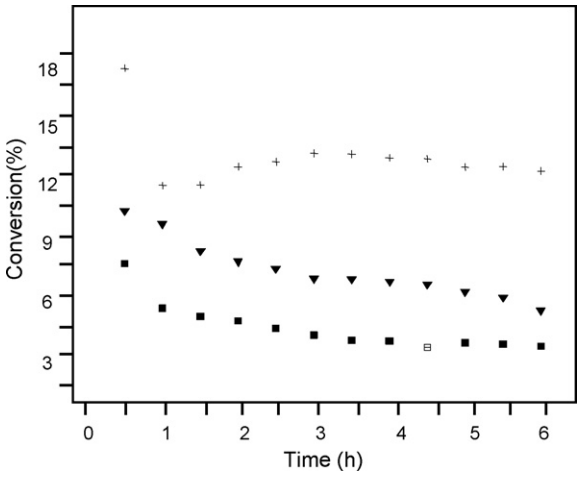

Fig. 4. Ethylbenzene conversion as a function of time on the catalysts prepared with ammonium hydroxide. F (■), LF01 (+) and LF02 (▼) samples: with molar ratio La/Fe = 0.1 and 0.2, respectively. Sample F: pure iron oxide.

also more active than a commercial catalyst, which led to 10% of ethylbenzene conversion and 9% of styrene yield (90% of styrene selectivity). With the aim of improving the catalytic properties of this solid, the effect of the kind of the precipitant agent, such as sodium hydroxide and sodium carbonate, on its properties was also studied.

The X-ray diffractograms of the solids obtained with different precipitant agent are shown in Fig. 5(a). It can be noted that the presence of sodium ions made the formation of big crystals easier, allowing the detection of hematite in the solids prepared with sodium hydroxide and sodium carbonate. After the catalytic evaluation, Fig. 5(b), all the samples showed the diffraction profile of magnetite.

The effect of the precipitant agent on the particle size was confirmed by Mössbauer spectroscopy. In all fresh catalyst (Table 3), a doublet was observed probably related to superparamagnetic hematite (α-Fe_2O_3). The solid prepared with ammonium hydroxide showed the smallest particle size. In this case, it is possible to see two magnetic components in the spectra, related to the core and to the shell of the particles. The sample precipitated with sodium hydroxide has the second smallest particle size while the solid prepared with sodium carbonate showed the biggest particle size. The Mössbauer parameter of the spent catalysts (Table 4) confirmed the presence of only magnetite, as observed by X-ray diffraction, in all the samples. The amount of Fe^{2+} species is much higher in the catalyst precipitated with sodium hydroxide, indicating that those materials are more reduced than those prepared with

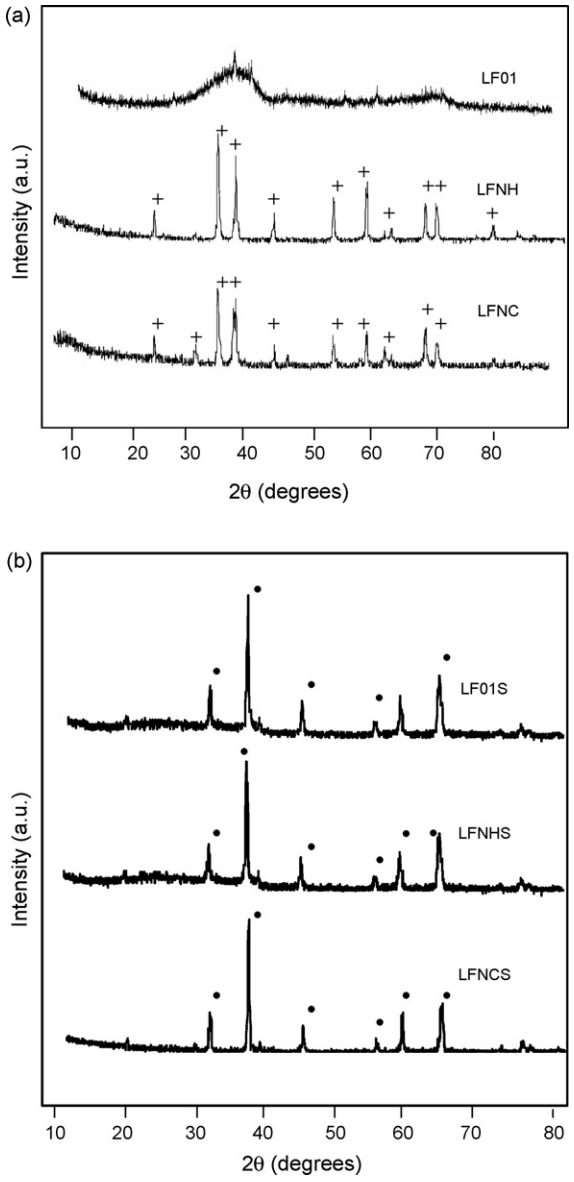

Fig. 5. X-ray diffractograms of fresh (a) and spent (b) catalysts prepared with different precipitant agents. LF01, LFNC and LFNH samples: with ammonium hydroxide, sodium carbonate and sodium hydroxide, respectively. (+) α-Fe_2O_3 and (●) Fe_3O_4.

ammonium hydroxide. In the case of the sample prepared with sodium carbonate, there was a sextuplet, whose isomeric shift at 0.19 ± 0.01 could not be identified.

In agreement with these results, the specific surface area of the solid prepared with ammonium hydroxide displayed the

Table 2
Ethylbenzene conversion (C), styrene selectivity (S_{ST}), benzene selectivity (S_B), toluene selectivity (S_T), styrene yield (Y_{ST}), activity (a) and activity per area (a/Sg) of the catalysts

Samples	C (%)	S_{ST} (%)	S_B (%)	S_T (%)	Y_{ST} (%)	$a \times 10^3$ (mol g^{-1} h^{-1})	a/Sg $\times 10^4$ (mol h^{-1} m^{-2})
F	4	92	5	3	4	3	3
LF01	13	88	7	5	11	10	10
LF02	7	83	9	8	6	5	4

LF01 and LF02 samples: with La/Fe (molar) = 0.1 and 0.2, respectively; F sample: pure iron oxide.

Table 3
Mössabuer parameters of the catalysts prepared with different precipitant agents

Species	Hyperfine parameter	LF01	LFNH	LFNC
α-Fe_2O_3 "core"	H (T)	50.26 ± 0.02	51.64 ± 0.07	50.80 ± 0.02
	δ (mm/s)	0.37 ± 0.01	0.37 ± 0.01	0.37 ± 0.03
	2ε (mm/s)	−0.19 ± 0.02	−0.20 ± 0.01	−0.20 ± 0.01
	%	45 ± 3	80 ± 2	87 ± 4
α-Fe_2O_3 "shell"	H (T)	47.8 ± 0.2	–	–
	δ (mm/s)	0.37 ± 0.01	–	–
	2ε (mm/s)	−0.19 ± 0.02	–	–
	%	35 ± 3	–	–
Possible α-Fe_2O_3 (sp)	Δ (mm/s)	0.70 ± 0.02	0.67 ± 0.01	0.77 ± 0.05
	δ (mm/s)	0.33 ± 0.02	0.34 ± 0.01	0.36 ± 0.04
	%	20 ± 2	20 ± 1	13 ± 3

LF01, LFNC and LFNH samples: with ammonium hydroxide, sodium carbonate and sodium hydroxide, respectively.

Table 4
Mössabuer parameters of the spent catalysts prepared with different precipitant agents

Species	Hyperfine parameter	LF01S	LFNHS	LFNCS
Fe^{3+} in Fe_3O_4	H (T)	49.10 ± 0.07	49.21 ± 0.02	52.2 ± 0.1
	δ (mm/s)	0.27 ± 0.01	0.29 ± 0.01	0.37 ± 0.01
	2ε (mm/s)	−0.01 ± 0.02	−0.01 ± 0.01	−0.07 ± 0.03
	%	19 ± 2	42 ± 2	8 ± 2
"$Fe^{2.5+}$" in Fe_3O_4	H (T)	45.87 ± 0.07	45.90 ± 0.03	49.05 ± 0.02
	δ (mm/s)	0.68 ± 0.01	0.66 ± 0.01	0.19 ± 0.01
	2ε (mm/s)	−0.01 ± 0.01	−0.01 ± 0.01	0.09 ± 0.01
	%	27 ± 2	49 ± 2	37 ± 2
Not known	Δ (mm/s)	0.61 ± 0.01	0.63 ± 0.03	0.55 ± 0.01
	δ (mm/s)	0.35 ± 0.01	0.34 ± 0.02	0.35 ± 0.01
	%	54 ± 2	9 ± 1	55 ± 2

LF01S, LFNCS and LFNHS samples: with ammonium hydroxide, sodium carbonate and sodium hydroxide, respectively.

highest value (Table 5), indicating that sodium ions favored the particle growing and then the decrease of specific surface area. After reaction, the specific surface area values remaining low, except the LF01 sample, which went on sintering.

The temperature-programmed reduction profiles of the solids prepared with different precipitant agents are shown in Fig. 6. It can be noted that the solids obtained with sodium carbonate or sodium hydroxide showed the low temperature peak (assigned to hematite reduction) shifted to higher temperatures, as compared to the sample obtained with ammonium hydroxide. It means that sodium ions made this process more difficult, independently of the anion (carbonate or hydroxide) of the precipitant. On the other hand, the solid prepared with sodium hydroxide displayed a significant decrease of the high temperature peak (due to metallic iron

Table 5
Specific surface area of the catalysts prepared with different precipitants before (Sg) and after the reaction (Sg*)

Samples	Sg ($m^2\ g^{-1}$)	Sg* ($m^2\ g^{-1}$)
LF01	115	10
LFNH	1.0	1.0
LFNC	1.0	2.0

Samples LF01, LFNC and LFNH: obtained with ammonium hydroxide, sodium carbonate and sodium hydroxide, respectively.

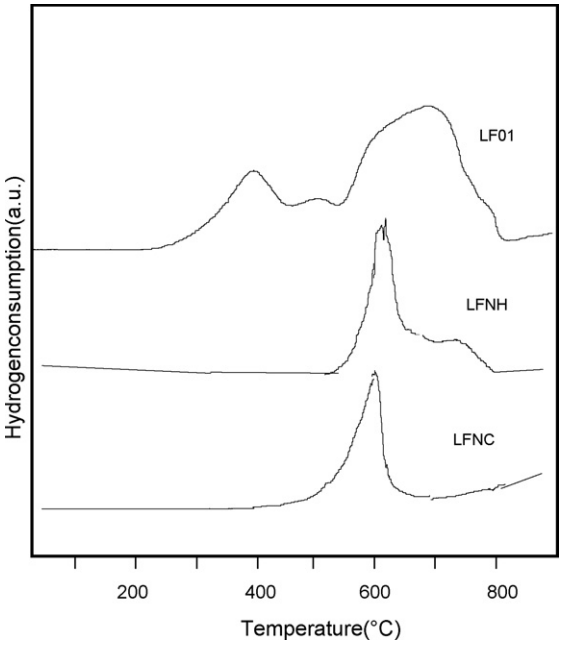

Fig. 6. Temperature-programmed reduction curves of the catalysts prepared with different precipitant agents. LF01, LFNC and LFNH samples: with ammonium hydroxide, sodium carbonate and sodium hydroxide, respectively.

Table 6
Ethylbenzene conversion (C), styrene selectivity (S_{ST}), benzene selectivity (S_B), toluene selectivity (S_T), styrene yield (Y_{ST}), activity (a) and activity per area (a/Sg) of the catalysts prepared with different precipitants

Samples	C (%)	S_{ST} (%)	S_B (%)	S_T (%)	Y_{ST} (%)	$a \times 10^7$ (mol g^{-1} s^{-1})	a/Sg $\times 10^8$ (mol m^{-2} s^{-1})
LF01	13	88	7	5	11	26	26
LFHN	4	72	15	13	3	2	16
LFCN	4	93	3	4	4	2	12

LF01, LFNC and LFNH samples: obtained with ammonium hydroxide, sodium carbonate and sodium hydroxide, respectively.

production), while the sample obtained with sodium carbonate did not show any peak, in this temperature range. This suggests an action of the anion from the precipitant agent (carbonate or hydroxide) on the reduction process (Fig. 6).

All catalysts were active and selective to styrene, in the ethylbenzene dehydrogenation in presence of steam, as shown in Table 6 and Fig. 7. Comparing the values of activity per area, it can be noted that sodium ions favored the production of less active catalytic sites. According to the Mössbauer results, these solids were more reduced than those obtained with ammonium hydroxide, after reaction. It means that these catalysts go on deactivation by the reduction of Fe^{3+} species (active phase) to Fe^{2+} species, during reaction [4,7]. It can also be noted that sodium carbonate increased the selectivity towards styrene while sodium hydroxide caused a decrease.

The presence of lanthanum on the solid surface was confirmed by X-ray photoelectron spectroscopy. Table 7 shows the binding energy of the core level of iron, lanthanum and sodium, which are in close agreement with those corresponding to the Fe^{3+}, La^{3+} and Na^{+} species [30]. The surface composition of the fresh catalysts showed that there was no lanthanum on the surface of the samples prepared with sodium carbonate, which explains its low specific surface area. Also, it can be noted that the surface was rich in sodium, that partiality covered the iron active sites. It means that the sodium species was not completely removed during the catalyst preparation. Comparing the fresh and spent catalysts, one can note that lanthanum

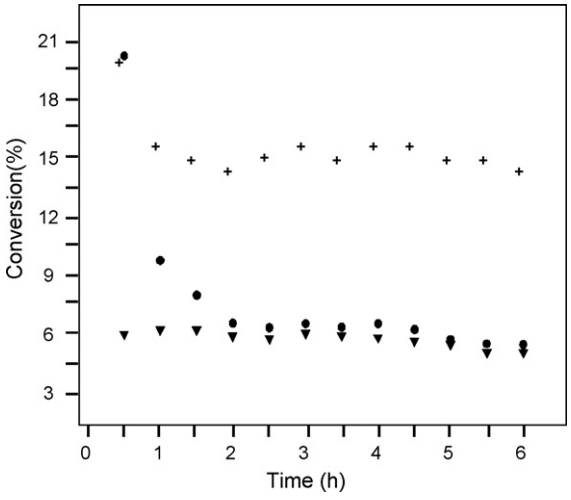

Fig. 7. Conversion as a function of time on the catalysts prepared with different precipitant agents. LF01 (+), LFNC (●) and LFNH (▼) samples: with ammonium hydroxide, sodium carbonate and sodium hydroxide, respectively.

Table 7
Binding energies (eV) and surface atomic ratios (La/Fe and Na/Fe) of the fresh catalysts. LF01, LFNC and LFNH samples: obtained with ammonium hydroxide, sodium carbonate and sodium hydroxide, respectively

Samples	Fe2p	La3d	O1s	Na1s	La/Fe	Na/Fe
LF01	713.1	837.1	532.2	–	2.839	–
LFNH	712.6	835.5	531.6	1074.1	2.160	11.527
LFNC	710.0	–	529.0	1071.1	0.0	26.155
LF01S	713.9	838.2	535.0	–	3.137	–
LFNHS	716.3	835.7	535.6	1073.7	0.0900	2.236
LFNCS	710.3	834.3	528.9	1071.2	0.0819	4.742

S represents the spent catalysts.

migrated to the surface (LFNC sample) or from the surface (LFNH sample) during the ethylbenzene dehydrogenation. In the LFNC sample, the lanthanum migration to the surface caused an increase of specific surface area. The amounts of sodium were higher than the iron ones on the catalysts surface, indicating that some active sites were covered by sodium species, explaining the low intrinsic activity of the catalysts. On the other hand, the surface of the solid prepared with ammonium hydroxide showed the highest amount of lanthanum, as compared to the other samples; this explains the high specific surface area of the fresh catalyst. During the ethylbenzene dehydrogenation, the particles of lanthanum oxide grew and lost their anti-sintering action, causing a decrease of the specific surface area of the spent catalyst. The presence of lanthanum on the surface also caused an increase of activity per area, which showed low values in the solids poor in lanthanum on the surface. From these results, it can be concluded that sodium has a negative effect on the specific surface area and on the catalytic activity of lanthanum-doped hematite. A similar result has been recently noted by An et al. [31] studying Fischer–Tropsch catalysts.

4. Conclusions

Lanthanum-doped hematite, prepared by precipitation techniques at room temperatures, is an active catalyst in ethylbenzene dehydrogenation in the presence of steam and is also selective to styrene. The most active catalyst is prepared using ammonium hydroxide and a lanthanum to iron molar ratio of 0.1. In this solid, lanthanum is mainly on the surface, where it avoids sintering, increasing the specific surface area of the solid. However, during the ethylbenzene dehydrogenation the lanthanum oxide particles grow and loss their anti-sintering action, causing a decreasing in the specific surface areas.

Lanthanum also contributes for increasing the activity per area, which is low in the other samples with few amounts of lanthanum.

The use of sodium hydroxide or sodium carbonate, instead of ammonium hydroxide, produces more reduced solids, with bigger particles and with lower specific surface areas. Sodium species are mainly on the surface, covering partially the iron active sites and causing a decrease in the catalytic activity.

Acknowledgements

MSS acknowledges CAPES for her scholarship and the authors acknowledge FINEP and CNPq for the financial support.

References

[1] J.A. Macia-Agulló, D. Cazorla-Amorós, A. Linares-Solano, U. Wild, D.S. Su, R. Schögl, Catal. Today 102 (2005) 248.
[2] X.M. Zhu, M. Schön, U. Bartmann, A.C. van Veen, M. Muhler, Appl. Catal. A: Gen. 266 (2004) 99.
[3] A. Sun, Z. Qin, J. Wang, Appl. Catal. A: Gen. 234 (2002) 179.
[4] F. Cavani, F. Trifiro, Appl. Catal A: Gen. 133 (1995) 219.
[5] N. Dulamiţă, A. Măicăneanu, D.C. Sayle, M. Stanca, R. Crăciun, M. Olea, C. Afloroaei, A. Fodor, Appl. Catal. A: Gen. 287 (2005) 9.
[6] I. Serafin, A. Kotarba, M. Grzywa, Z. Sojza, H. Bínczycka, P. Kústrowski, J. Catal. 239 (2006) 137.
[7] E.H. Lee, Catal. Rev. 8 (1973) 285.
[8] B.D. Herzog, H.F. Raso, Ind. Eng. Chem. Prod. Res. Dev. 23 (1984) 187.
[9] T. Hirano, Appl. Catal. A: Gen. 26 (1986) 81.
[10] G.R. Meima, P.G. Menon, Appl. Catal A: Gen. 212 (2001) 239.
[11] S.S.E.H. Elnashaie, B.K. Abdallah, S.S. Elshishini, S. Alkhowaiter, M.B. Noureldeen, T. Alsoudani, Catal. Today 64 (2001) 151.
[12] S.S.E.H. Elnashaie, B.K. Abdallah, R. Hughes, Ind. Eng. Chem. Res. 32 (1993) 2537.
[13] K. Fujimoto, T. Kunugo, Ind. Eng. Chem. Prod. Res. Dev. 20 (1981) 319.
[14] M.C. Rangel, J.R.C. Bispo, A.C. Oliveira, M.L.S. Correa, J.L.G. Fierro, S.G. Marchetti, Stud. Surf. Sci. Catal. 142 (2002) 517.
[15] M.C. Rangel, A.C. Oliveira, H.E.L. Bonfim, Quim. Nova 27 (2004) 247.
[16] M.C. Rangel, A.C. Oliveira, Quim. Nova 26 (2003) 170.
[17] M.C. Rangel, A.C. Oliveira, J.L.G. Fierro, A. Valentini, P.S.S. Nobre, Catal. Today 85 (2003) 49.
[18] M.C. Rangel, A.C. Oliveira, H.E.L. Bonfim, React. Kinet. Catal. 80 (2003) 359.
[19] A. Moronta, M.E. Troconis, E. González, C. Morán, J. Sánchez, A. González, J. Quiñónez, Appl. Catal. A: Gen. 310 (2006) 199.
[20] A. Miyakoshi, A. Ueno, M. Ichikawa, Appl. Catal. A: Gen. 216 (2001) 137.
[21] F.M. Bautista, J.M. Campelo, D. Luna, J.M. Marinas, R.A. Quirós, A.A. Romero, Appl. Catal. B: Environ. 70 (2007) 611.
[22] M.C. Rangel, F. Galembeck, J. Catal. 145 (1994) 364.
[23] R. Furuichi, M. Hachia, T. Ishii, Thermochim. Acta 133 (1988) 101.
[24] M. Tu, J. Shen, Y. Chen, Thermochim. Acta 302 (1997) 117.
[25] A. Neumann, D. Walter, Thermochim. Acta 445 (2006) 200.
[26] X. Wang, M. Wang, H. Wang, B. Ding, Mater. Lett. 60 (2006) 2261.
[27] H. Lin, Y. Chen ad, C. Li, Thermochim. Acta 400 (2003) 61.
[28] E. Rombi, I. Ferino, R. Monaci, C. Picciau, V. Solinas, R. Buzzoni, Appl. Catal. A: Gen. 266 (2004) 73.
[29] E.E. Unmuth, L.H. Achwartz, J.B. Butt, J. Catal. 61 (1980) 242.
[30] C.D. Wagner, W.M. Riggs, L.E. Davis, J.F. Moulder, G.E. Muilenberg, Handbook of X-ray Photoelectron Spectroscopy, PerkinElmer Coorporation, Eden Prairie, 1978, p. 46, 76, 132.
[31] X. An, B. Wu, W. Hou, H. Wan, Z. Tao, T. Li, Z. Zhang, H. Xiang, Y. Li, B. Xu, F. Yi, J. Mol. Catal. A: Chem. 263 (2007) 266.